



Ultra-low-loading pulsed-laser-deposited platinum catalyst films for polymer electrolyte membrane fuel cells



Waldemar Mróz^a, Bogusław Budner^a, Wojciech Tokarz^b, Piotr Piela^b,
Michael L. Korwin-Pawłowski^{c,*}

^a Institute of Optoelectronics, Military University of Technology, 2 Kaliskiego Street, 00-908 Warsaw, Poland

^b Industrial Chemistry Research Institute, 8 Rydygiera Street, 01-793 Warsaw, Poland

^c Université du Québec en Outaouais, Département d'informatique et d'ingénierie, 101 rue Saint-Jean-Bosco, Gatineau, Québec, Canada

HIGHLIGHTS

- Ultra-low loading (0.18–7.44 $\mu\text{g cm}^{-2}$) Pt catalyst for PEMFC was deposited by PLD.
- Power density 59.36 mW cm^{-2} at 1.24 $\mu\text{g cm}^{-2}$ of Pt on Nafion membrane was obtained.
- Power density 106.36 mW cm^{-2} at 1.24 $\mu\text{g cm}^{-2}$ of Pt on gas-diffusion layer obtained.
- Power density 188.44 mW cm^{-2} at 7.44 $\mu\text{g cm}^{-2}$ of Pt on gas-diffusion layer obtained.

ARTICLE INFO

Article history:

Received 18 June 2014

Received in revised form

9 September 2014

Accepted 26 September 2014

Available online 5 October 2014

Keywords:

Fuel cells

PEMFC

Pulsed laser deposition

Plasma modification

Platinum catalyst

ABSTRACT

In this work experimental results are presented and analyzed for catalytic platinum films of ultra-low thickness of 0.09–3.47 nm and Pt loading of 0.18–7.44 $\mu\text{g cm}^{-2}$ deposited using the PLD method with an ArF excimer laser ($\lambda = 193$ nm) at room temperature. For Pt deposited on the surface of the Nafion[®] membrane (electrolyte), in a fuel cell with PLD Pt working as oxygen cathode the peak power density is obtained equal to 59.36 mW cm^{-2} for the Pt loading of 1.24 $\mu\text{g cm}^{-2}$. In the case of Pt deposition on the gas-diffusion layer (as cathode), a much higher maximum power density of 106.36 mW cm^{-2} at the same loading and a maximum of 188.44 mW cm^{-2} at the 7.44 $\mu\text{g cm}^{-2}$ loading is observed. Experiments are also presented of Nafion[®] modification before the deposition of Pt on the Nafion[®], in which the surface of the membranes is enlarged by bombarding with Ar ions from a plasma generator of RF 13.56 MHz. The electrochemical activity of the elements prepared by PLD is assessed in a $\text{H}_2/\text{Pt}/\text{Nafion}^{\text{®}}/\text{Pt}/\text{O}_2$ PEMFC. The structure and morphology of the surface layers is examined by AFM and SEM microscopy.

© 2014 Elsevier B.V. All rights reserved.

1. Introduction

This work concerns fuel cells with ion conducting polymer membranes (PEMFC). The most important advantage of PEMFC is low temperature operation below 100 °C and the possibility of miniaturization, allowing their utilization in portable electronic equipment. The electrodes used in PEMFC are usually in the form of porous carbonized paper or of carbon fibre cloth impregnated from one side with a suspension of carbon in Teflon[®]. Between the electrodes there is an ion conducting membrane in the form of a thin polymer foil, most often Nafion[®]. Both sides of the membrane are covered with a platinum based catalyst and pressed on both

sides to the electrodes to obtain a good electric connection between the catalyst and the electrode and a large contact surface between the catalyst and the electrolyte [1].

In traditional implementations, thin films of catalyst are deposited on both sides of the polymer membrane as nanoparticles of platinum, unsupported or supported on an inert, conducting support for the cathode, and platinum–ruthenium for the anode [2–5]. Most often the catalyst films are applied from a suspension (a mixture of the catalyst and Nafion emulsion) by painting, sputtering, or similar application technique [3,6–9]. The amount of metal deposited that way usually ranges from 0.1 mg cm^{-2} in the case of hydrogen anodes to 4–6 mg cm^{-2} or more in the case of methanol anodes. Such an approach is not optimal, because its low effectiveness of catalyst utilization results in the increased cost of the fuel cell. The technical objective of this work was a substantial reduction of the quantity of Pt used without reducing the utility life

* Corresponding author.

E-mail address: michael.korwin-pawlowski@uqo.ca (M.L. Korwin-Pawłowski).

time of the cell as well as its efficiency [4,6,10–16]. One of the main directions of research on fuel cells is the application of plasma deposition methods allowing the deposition of catalyst films of even nanometric thickness [5,13,17–22,28] sometimes with designed molecular structure [19]. Sputtering [17–20,24,26] and also e-beam evaporation [31] have been used to deposit the catalyst films. If the catalyst is deposited as a thin film, it is important to accurately choose its thickness, which determines the type and amount of loss from active material placement as well as polarization losses in the cell [5]. The catalysts can be deposited directly on the Nafion membrane forming the cell electrolyte [5,8,20,23] or on the carbon-fibre gas-diffusion layer [13,18,19,24,25]. Attempts were also reported of simultaneous deposition of elements, like platinum and carbon, to obtain more efficient catalytic films [26]. Plasma deposition techniques were also used in conjunction with other methods, when thin films of catalyst were deposited on the catalyst layers formed by traditional methods (ink printing) [13]. Since the catalyst utilization in the fuel cell is determined mainly by the contact surface area of the catalyst with the Nafion electrolyte, the reduction of the thickness of the metal layer by an order of magnitude thanks to the use of plasma techniques can result in an improvement of the catalyst utilization and reduction of the fuel cells cost. Thus, plasma techniques allow improvement of the cell power per the mass unit of the catalyst [17]. Polarization curves presented by Schwanitz et al. [27] showed that to achieve the effectiveness of hydrogen oxidation at the level comparable to the commercial E-TEK electrode with $500 \mu\text{g cm}^{-2}$ of platinum it is sufficient to deposit a $3 \mu\text{g cm}^{-2}$ film of Pt. It was also observed that the increase of the effective loading of the Pt to $25 \mu\text{g cm}^{-2}$ significantly improved the durability of the anode. The electrodes with catalyst films deposited by plasma techniques proved themselves equally as oxygen-reducing cathodes [5,13,18,19,23,24,26,30] as well as hydrogen-oxidizing anodes [27]. Since the reaction of hydrogen oxidation in the cell is much more efficient than the reaction of oxygen reduction, it is not possible to compare directly the cells, in which the experimental electrode was the anode, to those, in which it was the cathode. In the case of the oxygen-reducing cathode the optimal amount of platinum was about $100 \mu\text{g cm}^{-2}$ [5,19,24]. Increasing the amount of platinum usually reduces the porosity of the deposited metal layer, which has a negative effect on the transport of the reagents and the products of the reaction [5]. However, much in this respect depends on the structure of the support used for sputtering. As apparent from the work of the 3M company [32], sputtering even considerable amounts of Pt ($150 \mu\text{g cm}^{-2}$) on a regular, nanostructured layer of crystalline, organic whiskers led to a cathode catalyst layer exhibiting absolute performance on par with a higher-loaded traditional PEMFC cathode. The initial problem of the 3M's nanostructured thin film (NSTF) electrodes was insufficient proton conduction in the film because ionomer was not introduced in the layer between the catalytic metal and the PEM [33]. This underlines the importance of designing an effective three-phase boundary in these catalyst layer fabrication techniques.

The method used in this work of pulsed laser deposition (PLD) of catalyst films in high vacuum conditions with an ArF laser allows precise control of the thickness and of the physicochemical structure of the fabricated films. The deposition in conditions of high vacuum also assures a high chemical purity of the films.

The research objective of the present work was the determination of the effects of the PLD process parameters on the physicochemical and electrochemical properties of the catalyst films deposited on off-the-shelf PEM fuel cell components. An important aspect of the work was to investigate if the laser deposition method would allow reducing the utilized amount of the noble metal, while

maintaining the efficiency of the cell or at least to increase the cell power obtained from a mass unit of the metal.

2. Experimental details

2.1. Pulsed laser deposition of platinum

The investigated catalyst was deposited by the pulsed laser ablation method using a Lambda Physik excimer laser LPX 305i at $\lambda = 193$, $E_L \leq 0.7$ J, $\tau \sim 15$ – 20 ns. Because of the low Nafion degradation temperature, the laser radiation fluency on the surface of the target disc did not exceed 14 J cm^{-2} . The pumping system allowed achieving an oil-free vacuum of $5.0 \cdot 10^{-5}$ mbar. The system included a 13.56 MHz RF plasma generator from the ENI Company and a gas dosing system for O_2 , N_2 , Ar and CH_4 . The catalyst was deposited from a $20 \times 20 \times 2$ mm platinum (99.99%at.) target. The thickness of the deposited Pt films was controlled by changing the number of the laser pulses. Because of differences in the roughness of the surfaces, on which the catalyst was deposited, we have introduced further in this work the concept of the effective thickness of the catalyst representing the thickness of the catalyst deposited on a polished silicon wafer with the same number of laser pulses.

In the first part of the investigation the catalyst films were deposited directly on the Nafion membranes. In order to increase the active area of the catalyst-electrolyte interface, some membranes were treated in 13.56 MHz argon plasma [2]. The modification process was conducted for different periods of time and RF generator power. The pressure in the experimental chamber was held during the modification process between $2.7 \cdot 10^{-2}$ and $9.0 \cdot 10^{-3}$ mbar. In an alternating electric field argon is ionized, which gives source to a stream of ions, electrons and UV radiation. The energy of ions used for the modification of the membranes depended mainly on the vacuum chamber pressure, on the geometry of the gas injection into the chamber, and on the gas flow. Depending on the conditions, the energy of ions could vary from a few tens to a few hundreds of electronvolts. The amount of energy transferred by the Ar^+ ions to a unit of the Nafion membrane surface is subject to large fluctuations and is difficult to estimate. The energy of the UV radiation in the present system was at least three times lower than the energy of the generated Ar^+ ions. Because the UV energy is emitted in the full solid angle, its contribution to the Nafion properties modification could be ignored, as was proven by Ramdutt et al. [2].

In the second part of investigations the Pt catalyst films were deposited directly on the gas-diffusion layer of the cathode structure. It was expected that the diffusion layer extending in three dimensions would assure a larger contact surface of Pt and the electrolyte and better transport conditions for the fuel and the oxidant compared to the deposition of the catalyst on the flat surface of Nafion.

2.2. Preparation of materials for the fuel cell

Platinum deposited by the PLD method was the cathode catalyst of the fuel cell. For the anode, a layer of platinum black (E-TEK, a division of De Nora North America Inc., Somerset, NJ, USA) was used, applied by painting [7] on the opposite side of the Nafion membrane (Nafion[®] 117, DuPont, USA). The anode ink was prepared in an ultrasonic mixer by mixing the platinum black powder with a 5% alcohol suspension of Nafion (Ion Power, USA) and double-distilled water. The composition of the ink was adjusted so as to obtain a volume ratio of 1:1 of the metal to solid Nafion in the dried catalyst layer. The fabricated membrane-electrode assembly (MEA) was mounted in house-designed fuel cell hardware. Carbon cloth

ELAT LT2500W (E-TEK) was used as the gas-diffusion layer (GDL) on both sides of the MEA. The geometric surface area of the painted-on anode was 5 cm^2 . The geometric surface area of the cathode made by the PLD method on the membrane was 4 cm^2 .

In the case of carbon cloth with PLD Pt films, before mounting the cloth in the cell, 1.5 mg cm^{-2} (dry basis) of Nafion was deposited on the Pt side from an alcohol suspension. The dried cloth was then attached by its catalyst and Nafion-covered side to the membrane using only the pressure of the cell fixture. The geometric surface area of the cathode fabricated in the described fashion was 5 cm^2 .

The deposition of platinum catalyst films on the surface of the membranes and on the carbon cloth was done under the range of pressures from $7.3 \cdot 10^{-5}$ to $2.7 \cdot 10^{-4}$ mbar. The electrochemical measurements performed did not show any appreciable effect of the pressure changes in the given range on the electrical characteristics of the MEA. The laser energy density on the Pt target surface was $13.4 \pm 0.6 \text{ J cm}^{-2}$. Electrodes were fabricated and tested with different equivalent catalyst film thicknesses ranging from 0.09 to 3.47 nm, proportional to the number of laser pulses from 75 to 3000.

The equivalent thicknesses of Pt films shown in Table 1 were determined as follows. Polished silicon wafers were cleaned with the laser (1000 laser pulses). Then, Pt was applied to these wafers by PLD under the conditions used for platinization of the fuel cell components. Three Pt depositions were done using three different numbers of laser pulses from $1.5 \cdot 10^4$ to $3.5 \cdot 10^4$ pulses. The numbers of pulses were selected as to obtain thicknesses of the Pt deposits much greater than the RMS roughness of the silicon substrate from AFM. The thickness of the deposited dense platinum layer was determined with AFM for each sample. This allowed calculation of the average mass of Pt landing on the substrate with each PLD pulse. This value multiplied by the number of pulses gave the equivalent thickness for the actual platinized fuel cell components. The estimated error of the equivalent thicknesses was $\pm 15\%$. The loadings of the Pt films in $\mu\text{g cm}^{-2}$ were calculated from the catalyst film thicknesses and the density of Pt (21.09 g cm^{-3}) from general physics tables.

2.3. Analytical equipment

The surface topographies of the deposited Pt films were visualized with an atomic force microscope (AFM) NanoScope IV of Veeco Inc. in the contactless tapping mode of operation. The analysis of the chemical composition of the RF-plasma-modified

Nafion membranes was done using an X-ray photoelectron spectroscope (XPS) with a R3000 VG Scienta (Sweden) analyzer and an X-ray tube with an Al K α cathode of Prevac Inc. (Poland). SEM imaging of the surfaces of the samples and energy-dispersive X-ray spectroscopy (EDS) elemental composition measurements were done with a Quanta 3D FEG microscope of FEI Company (USA). Electrochemical measurements on the fabricated catalyst films were done on a fuel cell test stand at the Industrial Chemistry Research Institute in Warsaw. The system controlling the fuel cell working conditions (cell temperature, flows, temperature, humidity and pressure of anode and cathode gases) was made in house. Cyclic voltammetry curves (CVs) were recorded with an SI 1287 electrochemical interface of Solartron Instruments (UK). Steady-state polarization curves and constant-voltage polarizations together with fuel cell internal resistances were recorded using a 6051A/60504B programmable DC electronic load (Agilent, USA), a 6031A programmable power supply (Hewlett–Packard, USA) and an SI 1260 impedance analyzer (Solartron Instruments). The internal resistances were measured at each point of a polarization curve by applying a 2-kHz sinusoidal load perturbation of 12 mA cm^{-2} amplitude (base-to-peak) and the resistance values reported are average values from all measurements at different loads (the load variability of the resistance was small). The high frequency used resulted in very small impedance phase angles for these fuel cells. For cells producing currents too low for the sensitivity of the 6051A/60504B and 6031A instruments, the polarization curves and constant-voltage polarizations were done using the SI 1287 instrument.

3. Results and discussion

3.1. Fabrication of the fuel cell components

The experimental parameters of films deposited on the electrodes and selected results of measurements are presented in Table 1. The essential feature of the electrodes prepared using PLD in this work were very low Pt loadings, which were two orders of magnitude lower than the loadings usually employed in the current PEMFC technology.

The AFM surface topography of the membrane not covered with a platinum film, presented on Fig. 1a, shows a very smooth surface of Nafion. The average root mean square of the surface roughness profile for the non-modified surface of the membrane was 3.6 nm. From the practical point of view such a low value is not

Table 1
Characteristics of the fabricated electrodes.

MEA#	Laser energy [mJ]	Number of laser pulses	Type of electrode, parameters of RF plasma surface modification	Cathode Pt loading [$\mu\text{g cm}^{-2}$]	Equivalent thickness of cathode Pt layer ($\pm 15\%$) [nm]	Average ohmic cell resistance [$\Omega \text{ cm}^{-2}$]	Maximum power density [mW cm^{-2}]	Maximum Pt utilization [W mg^{-1}]
1	285 ± 14	75 ± 5	Pt deposited on the membrane, 100 W, Ar $10 \text{ cm}^3 \text{ min}^{-1}$, $9.0 \cdot 10^{-3}$ mbar, 10 min	0.18	0.09	—	0.06	0.35
2	285 ± 14	150 ± 10		0.37	0.17	0.35	1.10	2.97
3	285 ± 14	300 ± 10		0.75	0.35	0.31	10.89	14.91
4	285 ± 14	500 ± 10		1.24	0.58	0.80	59.36	48.66
5	260 ± 10	1000 ± 10		2.48	1.16	—	14.00	5.74
6	265 ± 13	500 ± 10		1.24	0.58	0.80	42.19	34.59
7	265 ± 13	800 ± 10	Pt deposited on the membrane, 120 W, Ar $15 \text{ cm}^3 \text{ min}^{-1}$, $2.7 \cdot 10^{-2}$ mbar, 15 min + 15 min pause + 15 min	1.95	0.93	0.78	1.63	0.88
8	287 ± 14	500 ± 10	Pt deposited on the GDL	1.24	0.58	0.35	106.36	87.18
9	285 ± 14	1000 ± 10		2.48	1.16	0.37	146.02	59.84
10	285 ± 14	2000 ± 10		4.96	2.31	0.27	162.76	33.42
11	280 ± 14	3000 ± 10		7.44	3.47	0.22	188.44	25.78
12	—	—	Standard electrode with Pt black as cathode	4000.00	—	0.19	397.19	0.10

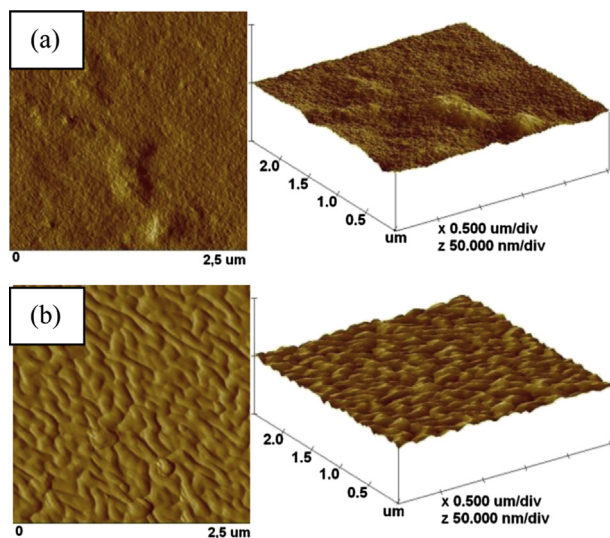


Fig. 1. AFM 2D and 3D images of the membrane surface: a) without Pt film, b) with deposited Pt film (2000 pulses, repetition 5 Hz, pressure $1.1 \cdot 10^{-4}$ mbar).

advantageous because it does not provide a large contact surface area of the membrane with the catalyst. The membrane covered with a platinum film of equivalent thickness of about 2.3 nm showed a not much higher roughness ($RMS = 7.2$ nm), resulting from a very good adhesion of Pt to the surface of the membrane and the typical uniform growth of the Pt film (Fig. 1b). Pt films deposited by the PLD method on the surface of unmodified Nafion membrane showed a high uniformity and covered very tightly the surface of the membrane. In practice, this is the main problem with the use of that method for the Pt/Nafion system. The same problem was encountered by R. O'Hayre et al. in the case of magnetron sputtering deposition of Pt [5]. They stated that the optimum thickness of sputtered Pt films was 5–10 nm and showed a maximum power output of about 23 mW cm^{-2} . We have observed a peak of power density of 59.36 mW cm^{-2} with much thinner PLD Pt films of 0.58 nm on the unmodified Nafion surface. Thicker films reduced the efficiency of the fuel cells because of the low porosity of the Pt film, which resulted in a slower transmission of the substrates and the increase of transport losses [19]. The Pt films best for fuel cells should have high porosity. The porous structure is a *sine qua non* condition for a high contact surface area of the catalyst with the electrolyte and at the same time an easy access of the reagents to the catalytically active region and the possibility of quick removal of the products of the reaction.

In order to increase the contact surface at the Pt–Nafion interface experiments were done aimed at enlargement of the Nafion membrane surfaces by subjecting them to argon plasma generated by 13.56 MHz RF energy. An example of such modification is shown on Fig. 2a. The modification of the membranes in a 13.56 MHz RF Ar plasma discharge significantly altered the structure of the surface. Depending on the used membrane modification conditions (time, generator power, pressure) different values of surface roughness were achieved. The value of the RMS roughness determined by AFM measurements of the sample shown on Fig. 2a is 46.8 nm, which is 13 times higher than for the non-modified sample. The maximum RMS roughness achieved was 162.8 nm by modification with RF power of $P_{RF} = 150 \text{ W}$ for 30 min at a pressure of $p = 3.6 \cdot 10^{-2}$ mbar. However, the increase of the roughness of the membrane surface by over an order of magnitude and an identical increase of the catalyst-to-polymer electrolyte contact surface area did not translate into an improvement of the parameters of the cells fabricated that way.

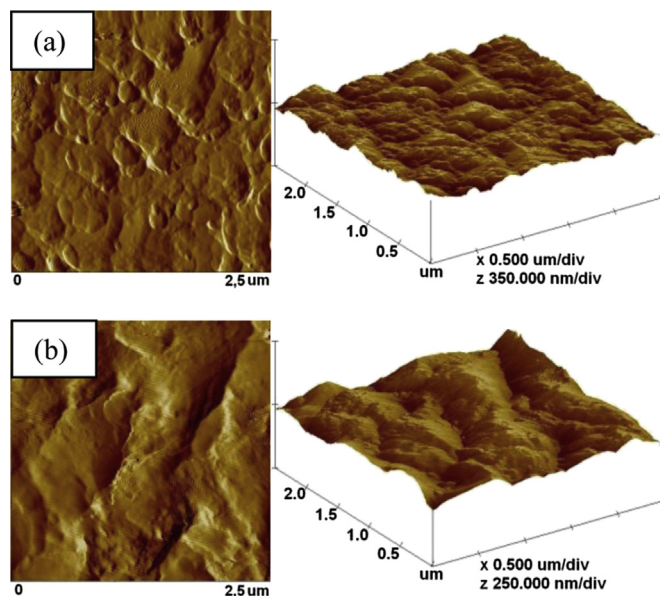


Fig. 2. AFM 2D and 3D images of the membrane surface: a) after Ar etching ($P = 150 \text{ W}$, $p = 1.7 \cdot 10^{-3}$ mbar, $t = 15 \text{ min}$), b) after Ar etching ($P = 150 \text{ W}$, $p = 1.7 \cdot 10^{-3}$ mbar, $t = 15 \text{ min}$) and coating with a film of Pt (500 pulses, repetition 10 Hz, pressure $1.7 \cdot 10^{-3}$ mbar).

Investigations of the Nafion surface to about 10 nm in depth into the material with X-ray photoelectron spectroscopy (XPS) indicated significant changes of the chemical structure of Nafion subjected to the argon plasma generated by 13.56 MHz RF. The unmodified material contained 66.0–69.1%at. fluorine, 1.6–3.2%at. oxygen, 28.1–30.7%at. carbon and about 0.2–0.3%at. sulphur. As a result of the modification the fluorine content dropped dramatically, even to 48.9%at., and the percent content of other elements increased, especially of oxygen (even by 10%at.), carbon (by about 7%at.) and sulphur (by up to 1.8%at.). Fig. 3 presents a comparison of C1s XPS bands of carbon for an unmodified membrane and for a membrane modified in RF Ar plasma. The change of the C1s band for the modified membrane proves that together with the change of the content of individual elements, the chemical structure of the material and changes of its polymer chain occur. On the surface of the

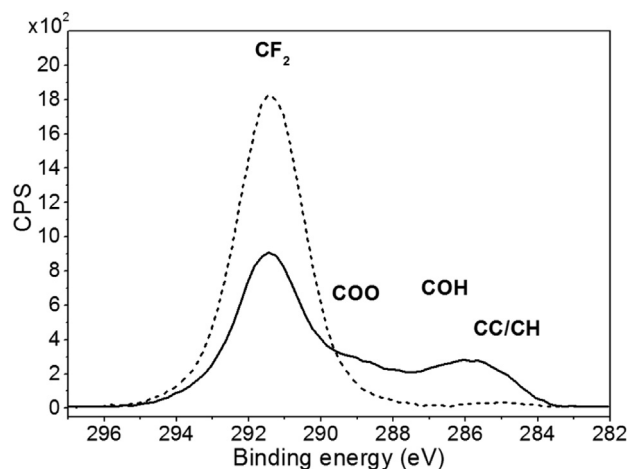


Fig. 3. Comparison of the 1s XPS bands of carbon for unmodified (dotted line) and modified Nafion membrane in argon RF plasma ($P = 25 \text{ W}$, $p = 3.8 \cdot 10^{-2}$ mbar, $t = 20 \text{ min}$) (solid line).

samples, there is a significantly reduced amount of the CF_2 functional groups and increased amount of COO, COH and CC/CH functional groups. As the results of electrochemical measurements show, the change of the polymer structure entails a reduction of ionic conductivity and leads to a reduction of the fuel cells efficiency [2]. XPS investigations prove that the used method of surface modification along with the desired effect of the development of the surface causes also a detrimental modification of the properties of the material. The results of the modifications of the membranes in RF plasma obtained by us are similar to the results of Ramdutt et al. [2], who have seen clear changes in the chemical structure of the polymer and a reduction of the efficiency of the fuel cells. Quite different were the results of modification of the membranes with an argon ion beam presented by M. Prasanna et al. [3], S. A. Cho et al. [4] and Y. H. Cho et al. [6]. Bombarding the surface of Nafion with a well characterized Ar ion beam from an ion gun, they obtained a significant development of the surface of the material (10 times increased RMS roughness) without a negative effect on its physicochemical properties and a doubling of the fuel cell power density for cells with modified membranes compared with those with non-modified membranes [4]. So, there exists a possibility of improving the efficiency of the fuel cells by Nafion surface modification using Ar ions as ion beams, even though Ar plasma ions treatment does not provide an improvement.

In the last stage of investigations Pt was deposited directly on the gas diffusion layer of the cathode. The deposition was done under similar conditions of pressure and laser energy density as for the case of Pt/Nafion (Table 1). To optimize the efficiency of the Pt/diffusion layer system and to compare it with the Pt/Nafion system a few catalyst films of different thicknesses were deposited proportionally to the numbers of laser pulses: 500, 1000, 2000 and 3000.

Because of the high porosity of the gas-diffusion microporous carbon layer (Fig. 4a) platinum does not form a continuous uniform film (Fig. 4b) and can, to a certain extent, penetrate into the porous structure of the substrate. That in turn can increase the active surface of the catalyst compared to the Pt/Nafion case. SEM images of the diffusion layer not covered with platinum and of the layer covered with platinum (Fig. 4) show only little differences of their structures. In the case of the diffusion layer covered with the catalyst a small increase of the surface structures can be observed. Platinum deposited by PLD forms a regular coating uniformly positioned on the surface of nanometric size particles constituting the upper surface of the diffusion layer. The structure of the diffusion layer allows a part of the deposited Pt to locate itself inside the visible pores. Therefore, in this case, before mounting the electrode in the cell, it was impregnated with Nafion in the form of a suspension, in order to obtain a large contact surface area of Pt to Nafion. Nafion in suspension form penetrates quite well into the void regions of the Pt-covered gas diffusion layer. The EDS measurement of the cross-section of the diffusion layer coated with Nafion (Fig. 5) allowed estimating the penetration depth of Nafion at about 20–30 μm on the basis of sulphur content, which is a component of Nafion, but is not present in the untreated diffusion layer.

3.2. The efficiency of fuel cells

Fig. 6 shows CVs of selected electrodes with Pt catalyst deposited by the plasma method. The curves were recorded before the first and after the tenth cycle of steady-state polarization curve recording and represent, in a way, an electrochemical snapshot of the fabricated catalyst films. The curves of Fig. 6a were obtained for a platinum electrode deposited directly on the membrane (MEA #4), which among the other electrodes of that group showed

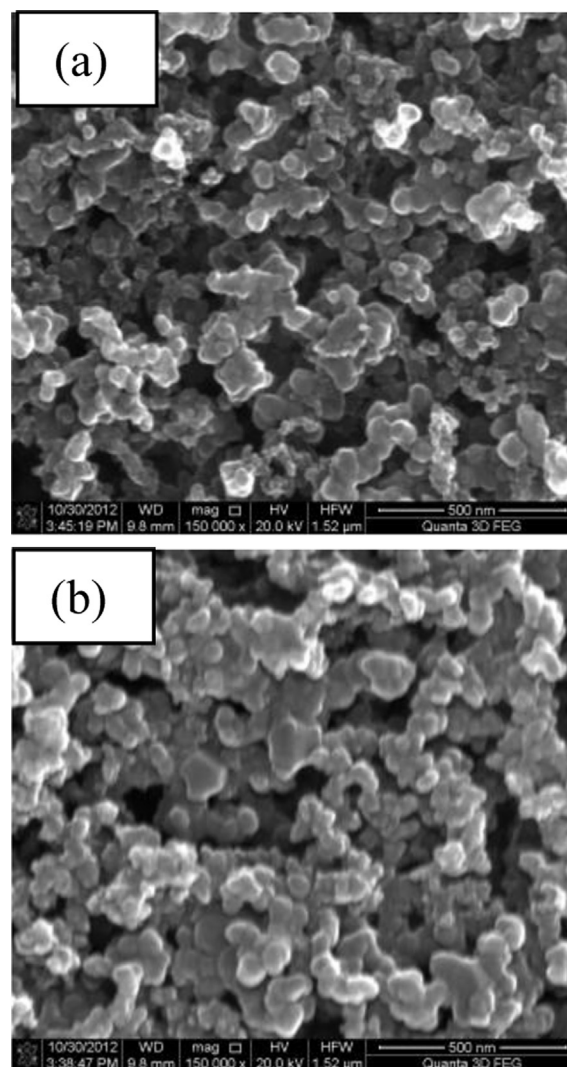


Fig. 4. SEM image of the top microporous layer of a carbon-fibre gas diffusion layer: (a) not covered by Pt (b) covered with Pt film (2200 pulses, repetition 10 Hz, pressure $3.1 \cdot 10^{-4}$ mbar).

highest current values, that is, had the highest electrochemically active surface area. The curve recorded before the first measurement cycle (solid line) has a tilted shape indicating a significant resistance caused most likely by a poor contact between the metal and the electrolyte (Nafion). All the characteristic regions representative of the surface processes occurring during the polarization of the electrodes, that is, electroadsorption and electrodesorption of hydrogen at low potentials (below 0.4 V), the double layer charging between 0.4 and 0.7 V and the peak around 0.8 V due to the reduction of the oxide layer formed above 0.7 V during the anodic scan, appear on the curve recorded after the 10th measurement cycle (symbolic line). Such a transformation of the catalyst film under polarization can be caused by migration of Nafion particles leading to an improvement of the metal-electrolyte contact. The possibility of an improvement of the electrical contact between the metal and the carbon cloth resulting from migration of platinum cannot be excluded, either.

The curves of Fig. 6b are the electrochemical snapshot of the surface of the electrode with the highest amount of platinum deposited on the gas diffusion layer (MEA #11). Even though the amount of deposited platinum is almost 6 times higher than for

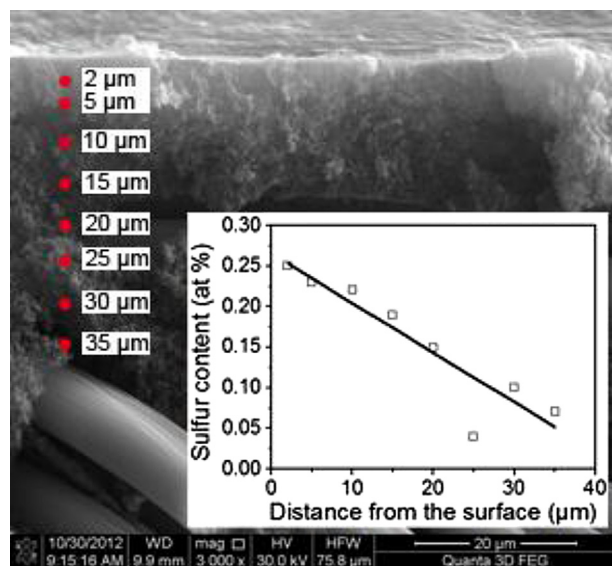


Fig. 5. SEM image of the cross-section of the gas diffusion layer impregnated with a Nafion suspension and a graph showing the dependence of the sulphur content as a function of the distance from the surface of the carbon layer.

MEA #4 (Fig. 6a), the recorded currents are two orders of magnitude lower. The dominant effect of the carbon substrate on the CV shape is also evident – a wide hysteresis on the first-cycle curve masks the platinum surface processes.

Paradoxically, in the case of deposition of Pt on the porous diffusion layer, the amount of the electrochemically active metal is much lower than in the case of direct deposition of platinum on the Nafion membranes, as evidenced by the lower area under the CV curve. This suggests that even though a continuous film of platinum is deposited on the surface of the membrane (see Fig. 1b and 2b), the metal during the sequential pulses of the laser can diffuse into the polymer, which leads to a significant increase of the Pt/Nafion contact surface area. A significant current of hydrogen evolution at the lowest potential values is indicative of the presence of platinum on the cathode of MEA #11. The rise of the hysteresis curve over the zero-current axis at low potentials is the result of transmission by the membrane of low amounts of hydrogen from the anode side (*hydrogen crossover*), which is then oxidized on the cathode side. The oxidation is only possible on platinum. The final CV shows a higher contribution of the platinum, which, similarly to the case of Pt deposited directly on the membrane, indicates a transformation of the catalyst film improving the contact between its components. During the operation of the cell it is the surface area of the Pt/Nafion contact that is principally increased, because the hysteresis width stays basically unchanged and the surface area of the carbon/Nafion contact is responsible for it. From the comparison of the CV curves for the electrodes with the Pt film deposited directly on the membrane and on the carbon cloth it follows that better metal-electrolyte contact and increase of the active platinum surface were achieved for the films deposited on the membrane.

More practical information on the operation of the fabricated catalyst films is provided by the polarization curves of the cells obtained by feeding them with pure hydrogen and pure oxygen (Fig. 7). Each point of the polarization curve represents a stationary state of the cell achieved after 60 s after establishment of the constant DC voltage on the cells terminals. The polarization curves allow evaluating the effects of the construction of the cell on the value of the activation losses, the resistive losses and the transport losses in the cell. The activation losses are the result of the need to

overcome the activation barriers of the electrode reactions. The ohmic resistive losses are caused by non-zero internal resistance of the cell. The mass-transport losses result from the resistance of the diffusion and convection of the substrates and products of the electrode reactions. All the three types of loss effects are present at each point of the polarization curve, but in the high cell voltage range the activation losses are dominant, in the intermediate voltage range (the linear section of the curve) it is the ohmic losses, and at low voltages it is the transport losses. In the case of cells with low electrochemically active surface of the catalyst the activation losses are large, which shows as a rapid drop of the voltage with the increase of current density in the low current density range. The cells with high internal resistance rapidly lose their voltage in the medium range of current density drawn from the cell. When the transport resistance is high, together with the reduction of voltage on the cell's terminals a situation rapidly develops that the substrates at the catalyst are exhausted, the products of the electrode reaction accumulate, and the current density cannot increase any more (limiting current). When activation and transport problems are severe, these phenomena significantly impact also the medium range of current density.

Fig. 7a shows polarization curves for cells with Pt deposited on the Nafion membrane. The individual cells differ by the amount of

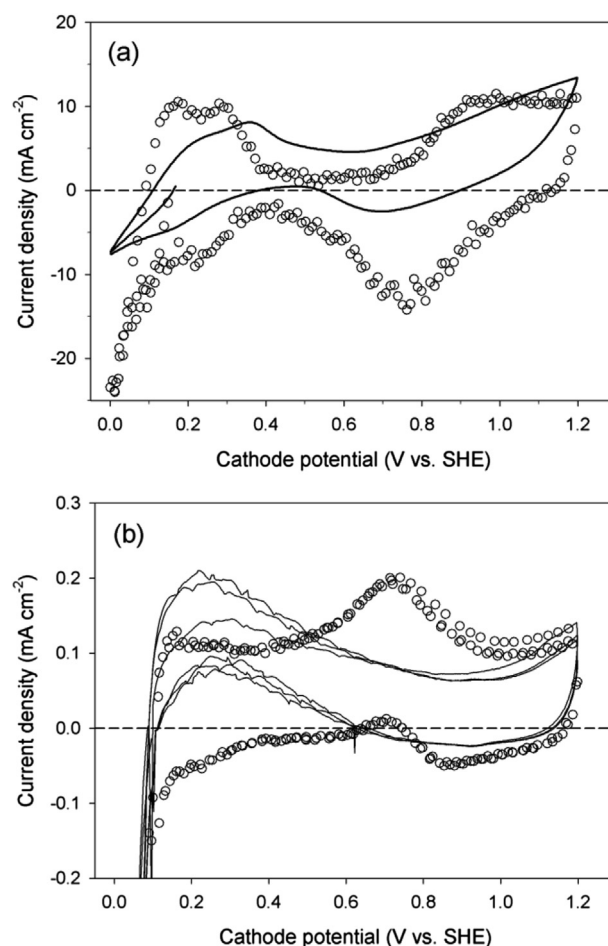


Fig. 6. Examples of cyclic voltammetry curves for MEAs with deposited Pt: a) directly on the MEA membrane MEA #4, b) on the gas diffusion layer MEA #11. Solid line – before the first cycle of polarization; symbolic line – after the tenth cycle of polarization. Scan rate 0.01 V s⁻¹. Recorded in fuel cell with humidified N₂ (cathode) and H₂ (anode) gas feeds at ambient temperature and pressure. Each curve shows three consecutive voltage cycles.

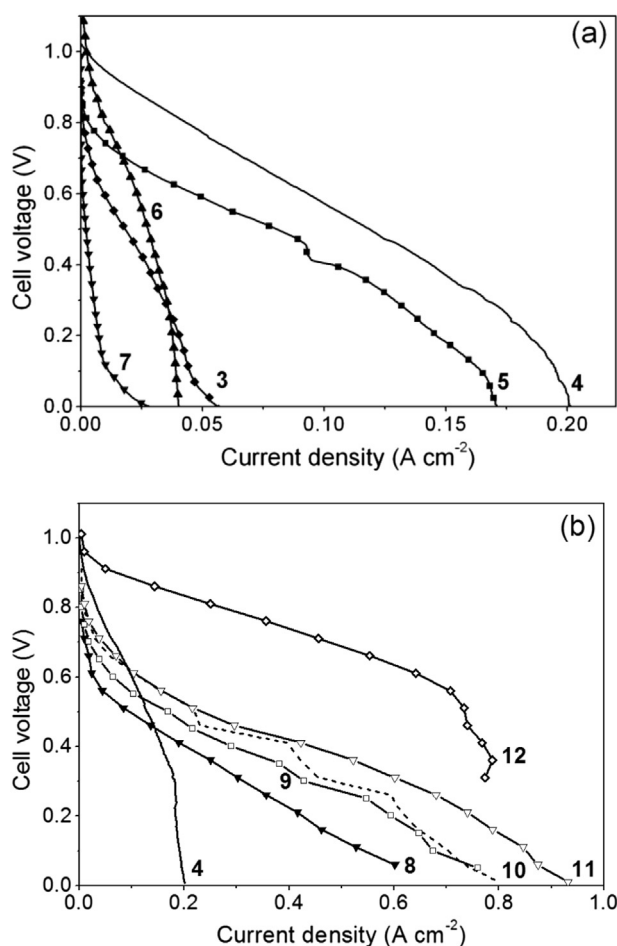


Fig. 7. Steady-state polarization curves for MEAs with Pt deposited directly on: a) membrane, b) gas diffusion layer (in reference to the painted-on cathode and best MEA with the Pt layer deposited on the membrane). The MEA numbers are according to Table 1. Measurements conditions: anode: H_2 , $300 \text{ Ncm}^3 \text{ min}^{-1}$, humidification 105°C , $240 \text{ kPa}_{\text{abs}}$, cathode: O_2 , $500 \text{ Ncm}^3 \text{ min}^{-1}$, humidification 95°C , $240 \text{ kPa}_{\text{abs}}$. Cell temperature 80°C .

platinum deposited and, in the case of MEA #6 and #7, also by the application of membrane surface enlargement described in section 3.1. The effect of the amount of deposited platinum can be followed analyzing the curves from 3 to 5. Curve 3 corresponds to the electrode with $0.75 \mu\text{g cm}^{-2}$ platinum. In the region of the highest values of the cell voltage, the slope of that curve is the highest among the 3 considered MEAs. This is the result of a large activation resistance of the cathode reaction due to the low platinum loading. The largest loading of platinum in the group of MEA #3 to MEA #5 is in MEA #5. That cell works better than MEA #3 in the kinetic range of the polarization curve (the range of the highest cell voltages), but not as well as MEA #4, the cathode of which has a twice lower platinum loading. This shows that too high an amount of platinum deposited on the membrane leads to a reduction of the electrochemically active surface area of the electrode. PLD deposition of an overly high amount of Pt on the membrane clearly leads to a spoiling of the Pt/Nafion interface formed during the initial laser pulses. In turn, in the region of higher current densities, where the internal resistance and the transport of the reagents start dominating, all 3 MEAs (#3, #4 and #5) reveal limitations clearly due to transport effects. This is because the internal resistances are of the same order, and the associated voltage drops small enough, so they cannot explain the high polarization of the cells. The

increase of the transport losses stems from the bulk character of the deposited Pt films. With the increase of their thickness the access of the substrates to the electrochemically active region, which is the Pt/Nafion interface, and the evacuation of the reaction products start getting restricted.

The effect of the enlargement of the surface of the membranes and electrodes by RF argon plasma etching is shown on curves 6 and 7. Those MEAs differ from each other by the total energy transferred to the membrane during the plasma processing. In the case of low-energy processing, the polarization curve (Fig. 7a, MEA #6) shows a difference from the curve for the most active electrode with the same platinum loading (Fig. 7a, MEA #4), which indicates an increase of the activation and transport resistances (the ohmic resistance remaining unchanged, see Table 1). The increase of the energy transferred to the membrane from the plasma leads to an almost complete loss of the cell's ability to convert energy, the larger amount of platinum notwithstanding (Fig. 7a, MEA #7). That means, the RF argon plasma leads to the loss of the Nafion's ability for conducting protons in a thin surface layer of the membrane subjected to the interaction with the plasma. That region is in contact with the catalyst, which, however, cannot be active because the access to it is limited for the protons – the substrates of the cathodic electrode reaction. The region of the limited proton conduction is thin enough not to affect the overall internal resistance of the cell (Table 1). A similar tendency of reduction of the cell efficiency with the increase of the energy provided by the RF plasma was observed by Ramdutt et al. [2].

The cells with platinum deposited on the gas-diffusion layer are characterized by much higher maximum current densities than the cells with platinum deposited on the Nafion membranes. The polarization curves of those cells are presented in Fig. 7b. The advantage of depositing platinum directly on the carbon cloth is in the improvement of the reagents transport in the region of the electrode reaction. At low cell voltages the cell currents are high, which tells that the transport resistance is low, even lower than for the standard cell with a high platinum loading (Fig. 7b, MEA #12). Also, the ohmic losses dominating in the medium voltage range are lower than the corresponding losses in the cell with Pt deposited on the membrane (Table 1). However, in the case of cells with Pt deposited on the GDL the problem of significant activation losses still remains. In the range of high cell voltage, the cathodes generate lower currents than the cathodes with Pt deposited on the membranes because of the lower active surface area of the catalyst (cf. Fig. 6a and b). It seems important to refine the process of Nafion coating the GDL with the platinum deposited on it. Increasing the platinum loading on the cloth by increasing the number of laser pulses brings clear effects until about $2 \cdot 10^3$ pulses (MEAs #8–11). Above that value there is no significant improvement of the efficiency of the cathode in the kinetic region.

A detailed comparison of the MEAs performance is possible by analyzing the curves of the power densities of Fig. 8 and the values of the maximum power densities together with the calculated platinum utilizations presented in Table 1. In the group of cells with platinum deposited on the membrane, the highest output power density per electrode surface area is 59.36 mW cm^{-2} for MEA #4. In the case of thinner or thicker catalyst films, the Pt utilization drops dramatically, which is due to a too small amount of catalyst or to the formation of too tight a layer. The maximum power density for MEA #4 in relation to the standard electrode with platinum black is almost 7 times lower (Table 1), but the Pt utilization is much higher for the PLD Pt deposition method: 0.10 W mg^{-1} for the standard electrode and 48.66 W mg^{-1} for MEA #4. Even if the platinum loading were reduced from 4.0 mg cm^{-2} to 0.4 mg cm^{-2} [8] for the reference cathode #12, which could be done without compromising the power density, the expected platinum utilization

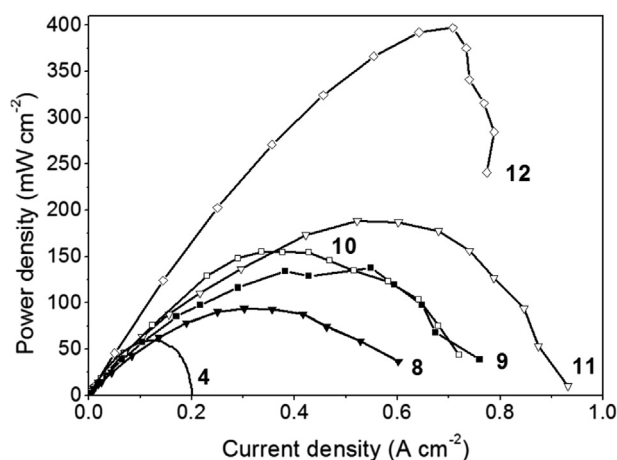


Fig. 8. Steady-state power density curves for selected MEAs. The MEA numbers are according to Table 1 (4 = best MEA with Pt deposited on membrane, 8 to 11 = MEAs with Pt deposited on GDL in increasing amounts, 12 = reference MEA with high-loading Pt black cathode).

(assuming that the cell output power would not decrease) would increase to about 1.0 W mg^{-1} , which would be still very low compared to MEA #4.

Much better results, in terms of maximum power density, were obtained for MEAs with the catalyst deposited on the carbon cloth. Comparing MEA #4 (Pt on Nafion membrane) and MEA #8 (Pt on cloth) having the same platinum loading, MEA #8 shows an almost double maximum power density and effectiveness of utilization of Pt. From the above analysis it can be concluded the MEA maximum power density and effectiveness of platinum utilization results from low ohmic and transport losses, because MEA #8 has a twice lower ohmic resistance compared to MEA #4 (Table 1) and much lower transport losses.

In the group of cells with the catalyst deposited on the GDL one can observe a clear drop of the cell resistance with the increase of catalyst loading (cf. MEA #8 – MEA #11). At the same time, because of the high porosity of the platinum film deposited on the gas diffusion layer, one does not observe any reduction of the maximum output power density of the cells in the investigated catalyst loading range. The highest maximum output power density $188.44 \text{ mW cm}^{-2}$ was achieved on MEA #11, the cathode of which was covered with a Pt film of 3.47 nm equivalent thickness. With the increase of the equivalent thickness, however, the platinum utilization drops (Table 1) from 87.18 W mg^{-1} for MEA #8– 25.78 W mg^{-1} for MEA #11. With increased number of laser pulses platinum locates itself on the surfaces of the structures visible in Fig. 4, contributing mainly to the increase of the Pt deposit thickness, while only a small part of platinum reaches into the visible pores where they would contribute to the increase of the active interface on the catalyst-electrolyte contact. Therefore, a change of the GDL pore dimensions and of their density could result in an increase of the active surface area of the catalyst-electrolyte contact.

It is important to note that not only a high Pt utilization is needed but also the absolute performance of PEMFCs (W cm^{-2}) needs to be high to result in a low fuel cell stack cost, a high power from unit volume, and, last but not least, a high efficiency of energy conversion. Even the best MEAs prepared in this work do not match the present PEMFC state-of-the-art in absolute performance, although they still carry ca. two orders of magnitude less Pt on the cathode. Further work is needed on the physical methods of catalyzing PEM MEAs.

4. Conclusions

The application of the PLD technique to the deposition of platinum allows fabrication of catalyst films with precisely controlled low metal loadings and high uniformity. The fuel cells utilizing platinum films of nanometric thickness show much higher platinum utilizations ($\text{W mg}^{-1} \text{ Pt}$), even a few to a few tens of times higher compared with electrodes prepared by traditional application methods. However, they show significantly lower maximum output power densities.

The efficiency of the fuel cells with PLD-deposited catalyst layers should be improved by increasing the catalyst-electrolyte contact area and by optimizing further the reaction region to improve the transport of reagents. Two approaches to do this were tested in this work: enlargement of the membrane surface area and deposition of Pt on the microporous surface of the GDL.

The method we used for enlarging the surface of the membranes by discharging a 13.56 MHz RF generator in the argon plasma did not prove itself, in spite of significant increase of surface roughness, because of ensuing degradation of the chemical structure of Nafion. Possibly, that problem could be avoided by using an ion beam with precisely adjusted energy for modification of the Nafion's surface. On the other hand, the membrane may be too soft a material for etching and in this way obtaining a radical increase of the electrode's three-phase boundary.

The deposition of the catalyst directly on the GDL yielded a several times higher maximum current density of the fuel cell and more efficient utilization of platinum than in the case of deposition of the catalyst on the Nafion surface. The main reason of the improvement is the higher porosity of the GDL. The catalytic layers forming in the GDLs are characterized by very good transport properties and by low resulting fuel cell internal resistances. Requiring improvement is the active Nafion-catalyst contact surface area, which is too low. A certain improvement could, perhaps, be achieved by optimizing the size of the pores and the dimensions of the surface structures, while preserving the reactant transport properties of the GDL. The effort done by 3M with their NSTF [32] is a similar approach of finding the right structure of the support for sputtering a catalytic material. The NSTF MEAs' absolute performance is significant and proves the strategy is viable.

As a result of the increase of the surface to bulk ratio, thin film catalysts deposited by plasma techniques have potential for a higher utilization of the noble metal in terms of watts per milligram of platinum, compared with traditionally prepared platinum nanoparticle catalysts. Yet, to improve the absolute performance of these thin films a break-through preparative approach is needed. It should be recognized the physical deposition techniques are spray techniques, in which the material deposits principally on the facets of the support that are perpendicular to the direction of the spray. This feature somehow limits the possibility of preparing catalyst layer structures with desired properties by spraying an already fully structured support. New, promising methods of further improvement of the physically deposited catalyst layer performance have recently been proposed, among them methods using various types of carbon carriers decorated with metal catalysts and multilayered cathodes [29,34,35].

Acknowledgements

The presented work was financed by the Ministry of Science and Higher Education of Poland through project #3135/B/T00/2010/38 "Membrane-electrode assemblies implanted with catalyst materials at the subsurface region using PLD for fuel cells". The authors thank Ms. Barbara Korzyc for the SEM investigations and Ms. Sylwia Budryńska for performing the AFM investigations.

References

- [1] W. Vielstich, A. Lamm, H.A. Gasteiger (Eds.), *Handbook of Fuel Cells: Fundamentals, Technology, Applications, Fuel Cell Technology And Applications: Part 1, Part 3: Polymer Electrolyte Membrane Fuel Cell Systems (PEMFC), Membrane-Electrode-Assembly (MEA)*, vol. 3, John Wiley & Sons, Chichester, 2003.
- [2] D. Ramdutt, C. Charles, J. Hudspeth, B. Ladewing, T. Gengenbach, R. Boswell, A. Dicks, P. Brault, *J. Power Sources* 165 (2007) 41–48.
- [3] M. Prasanna, E.A. Cho, H.-J. Kim, T.-H. Lim, I.-H. Oh, S.-A. Hong, *J. Power Sources* 160 (2006) 90–96.
- [4] S.A. Cho, E.A. Cho, I.-H. Oh, H.-J. Kim, H.Y. Ha, S.-A. Hong, J.B. Ju, *J. Power Sources* 155 (2006) 286–290.
- [5] R. O'Hayre, S.-J. Lee, S.-W. Cha, F.B. Prinz, *J. Power Sources* 109 (2002) 483–493.
- [6] Y.-H. Cho, J.W. Bae, Y.-H. Cho, J.W. Lim, M. Ahn, W.-S. Yoon, N.-H. Kwon, J.Y. Jho, Y.-E. Sung, *Int. J. Hydrogen Energy* 35 (2010) 10452–10456.
- [7] R. Bashyam, P. Zelenay, *Nature* 443 (2006) 63–66.
- [8] R.R. Passos, V.A. Paganin, E.A. Ticianelli, *Electrochim. Acta* 251 (2006) 5239–5245.
- [9] Y. Qiu, H. Zhang, H. Zhong, F. Zhang, *Int. J. Hydrogen Energy* 38 (2013) 5836–5844.
- [10] J. Zhang, M. Huang, H. Ma, F. Tian, W. Pan, S. Chen, *Electrochim. Commun.* 9 (2007) 1298–1304.
- [11] Y. Liang, H. Zhang, B. Yi, Z. Zhang, Z. Tan, *Carbon* 43 (2005) 3144–3152.
- [12] E. Antolini, *Appl. Catal. B: Environ.* 123–124 (2012) 52–68.
- [13] C.-H. Wan, Q.-H. Zhuang, *Electrochim. Acta* 52 (2007) 4111–4123.
- [14] J.N. Wang, Y.Z. Zhao, J.J. Niu, *J. Mater. Chem.* 17 (2007) 2251–2256.
- [15] A. Brouzgou, S.Q. Song, P. Tsiakaras, *Appl. Catal. B: Environ.* 127 (2012) 371–388.
- [16] S.H. Cho, H.N. Yang, D.C. Lee, S.H. Park, W.J. Kim, *J. Power Sources* 225 (2013) 200–206.
- [17] S.K. Natarajan, J. Hamelin, *J. Power Sources* 195 (2010) 7574–7577.
- [18] Y.-C. Lai, K.-L. Huang, C.-H. Tsai, W.-J. Lee, Y.-L. Chen, *Int. J. Energy Res.* 36 (2012) 918–927.
- [19] K.-L. Huang, Y.-C. Lai, C.-H. Tsai, *J. Power Sources* 156 (2006) 224–231.
- [20] I. Chang, S. Woo, M.H. Lee, J.H. Shim, Y. Piao, S.W. Cha, *Appl. Surf. Sci.* 282 (2013) 463–466.
- [21] H.-T. Kim, D.J. You, H.-K. Yoon, S.H. Joo, C. Pak, H. Chang, I.-S. Song, *J. Power Sources* 180 (2008) 724–732.
- [22] J.-H. Wee, K.-Y. Lee, S.H. Kim, *J. Power Sources* 165 (2007) 667–677.
- [23] S.Y. Cha, W.M. Lee, *J. Electrochem. Soc.* 146 (1999) 4055–4060.
- [24] S. Hirano, J. Kim, S. Srinivasan, *Electrochim. Acta* 42 (1997) 1587–1593.
- [25] J. Li, F. Ye, L. Chen, T. Wang, J. Li, X. Wang, *J. Power Sources* 186 (2009) 320–327.
- [26] M. Cavarroc, A. Ennadjaoui, M. Mougnot, P. Brault, R. Escalier, Y. Tessier, J. Durand, S. Roualdes, T. Sauvage, C. Coutanceau, *Electrochim. Commun.* 11 (2009) 859–861.
- [27] B. Schwanitz, H. Schulenburg, M. Horisberger, A. Wokaun, G.G. Scherer, *Electrocatal* 2 (2011) 35–41.
- [28] R. Eason (Ed.), *Pulsed Laser Deposition of Thin Films*, Wiley-Interscience, New York, 2007.
- [29] S. Zhang, X.-Z. Yuan, J. Ng Cheng Hin, H. Wang, K.A. Friedrich, M. Schulz, *J. Power Sources* 194 (2009) 588–600.
- [30] Zh Jiang, Zh-J. Jiang, *J. Membr. Sci.* 456 (2014) 85–106.
- [31] M.A. Raso, I. Carillo, E. Mora, E. Navarro, M.A. Garcia, T.J. Leo, *Int. J. Hydrogen Energy* 39 (2014) 5301–5308.
- [32] M.K. Debe, in: W. Vielstich, A. Lamm, H.A. Gasteiger (Eds.), *Handbook of Fuel Cells: Fundamentals, Technology, Applications*, John Wiley & Sons, New York, 2003, p. 576.
- [33] P.K. Sinha, W. Gu, A. Kongkanand, E. Thompson, *J. Electrochem. Soc.* 158 (2011) B831–B840.
- [34] D. Fofana, S.K. Natarajan, J. Hamelin, P. Bernard, *Energy* 64 (2014) 398–403.
- [35] A. Bonnefont, P. Ruvinskiy, M. Rouhet, A. Orfanidi, S. Neophytides, E. Savinova, *Wiley Interdisciplinary Reviews: Energy and Environment*, 2014. <http://dx.doi.org/10.1002/wene.110>.